NYU-AA-66-66

EFFECTS OF NOSE BLUNTNESS ON THE BOUNDARY LAYER CHARACTERISTICS OF CONICAL BODIES AT HYPERSONIC SPEEDS

Nicholas R. Rotta

This work was supported by:
Department of the Navy
Office of Naval Research
Contract NONR285(63)

November 1966

New York University
School of Engineering and Science
University Heights, New York, N.Y. 10453

Research Division
Department of Aeronautics and Astronautics

NYU-AA-66-66

EFFECTS OF NOSE BLUNTNESS ON THE BOUNDARY LAYER CHARACTERISTICS OF CONICAL BODIES AT HYPERSONIC SPEEDS

Nicholas R. Rotta

New York University
Bronx, N. Y.

November 1966

This work was supported by:
Department of the Navy
Office of Naval Research
Contract NONR285(63)

FOREWORD

This report was prepared by Mr. Nicholas R. Rotta, Research Assistant. The contract number under which this investigation has been carried out is NONR285(63) entitled, "Analytical and Experimental Investigations of Viscous Interactions at Low Reynolds Numbers".

ABSTRACT

The effect of nose blunting on the boundary layer characteristics over the conical part of a body is investigated. The boundary layer parameters $\bar{\delta}^*$, $\bar{\theta}$, $R_{e\theta}$, $N_u/(R_{eol})^{\frac{1}{2}}$ are found as functions of the similarity parameter $\bar{s}/R_{e\infty}^{1/3}$, and the boundary layer equations are integrated numerically. The resulting profiles are general, being independent of unit freestream Reynolds number and nose radius. The effect of bluntness on transition is investigated. Using the variation of Reynolds number based on the momentum thickness in the swallowing region as an indicator, the type of transition likely to occur, i.e., blunt body $R_{e\theta T} \approx 340$ or conical transition $R_{e\theta T} \approx 700$, is examined. The range of unit freestream Reynolds number for which conical transition will occur is identified specifically for the family of blunted conical bodies of 8° half angle at Mach 10. Based on the transition data, the heat transfer is calculated for regions of the swallowing process for which the boundary layer is laminar.

The results indicate a reduction of heat transfer is associated with nose bluntness and can be significant downstream of the nose region if the body nose radius is chosen to make the swallowing distance approximately twice that of the body surface length.

TABLE OF CONTENTS

LIST OF FIGURES

List of Figures (continued)

LIST OF SYMBOLS

a	defined by Eq. 8
A	constant by integration Eq. 12
B	ratio: $R_{e\infty}/R_{eol}$
C_p	specific heat at constant pressure
C_{dT}	drag coefficient of spherical nose
D	$\left[\frac{u_\infty \rho_\infty \mu_\infty}{(h_{ol})^{\frac{1}{2}} \rho_{ol} \mu_{ol}}\right]^{-\frac{1}{2}}$
f	transformed stream function
g	h_o/h_{oe}
h	enthalpy
j	defined by Eq. 13
k	thermal conductivity coefficient
M	Mach number
N_u	Nusselt number $\equiv \frac{C_{poe} R_o q_w'}{k_{oe}(h_{oe}-h_{ow})}$
P	pressure
$\dot{q}$	heat transfer rate
P_r	Prandtl number $\equiv \frac{C_p \mu}{k}$
R	gas constant
r	radial body coordinate
R_o	nose radius
$R_{e\infty}$	Reynolds number $\frac{\rho_\infty u_\infty R_o}{\mu_\infty}$
R_{eol}	Reynolds number $\frac{\rho_{ol}(h_{ol})^{\frac{1}{2}} R_o}{\mu_{ol}}$
R_{eos}	Reynolds number $\frac{\rho_{ol}(h_{ol})^{\frac{1}{2}} s}{\mu_{ol}}$

s'	distance along body surface from the stagnation point
$\bar{s}'$	s'/R_o
S	distance along body surface measured from the sharp cone vertex
$\bar{S}$	S/R_o
S_c	swallowing distance
γ	ratio of specific heats
δ_c	conical shock angle
$\bar{\delta}^*$	normalized boundary layer displacement thickness, δ/R_o
η	Lees transverse coordinate
θ_B	cone half angle
$\bar{\theta}$	normalized momentum thickness, θ/R_o
μ	dynamic viscosity
ρ	density

Subscripts

o	stagnation conditions
e	local conditions at boundary layer edge
c	inviscid sharp cone conditions
∞	freestream conditions
1	conditions behind normal shock
s	conditions corresponding to blunted cone shoulder
T	conditions corresponding to boundary layer transition
w	conditions at the body surface
-	overbar denotes non-dimensionalization with respect to R_o, or freestream conditions

INTRODUCTION

The entropy layer caused by the curved shock associated with nose blunting provides a rotational external stream through which the boundary layer develops. As pointed out by Ferri and Libby[1] the interaction between the rotational external flow and the viscous flow near the wall may in some instances invalidate the classical boundary layer approach This interaction effect becomes important when the vorticity of the external stream is on the same order as the average vorticity in the boundary layer (Ref 2) These conditions may exist for example in the combination of low Reynolds number (low boundary layer vorticity) and high Mach number (high external stream vorticity due to the highly curved shock). This problem was investigated for heat transfer in the nose region in Ref. 3 and it was found that a modification of the classical boundary layer external boundary conditions was necessary to satisfactorily describe the flow, even at very low Reynolds numbers At higher Reynolds number the effect of the free-stream vorticity on the boundary layer profile becomes negligible and the results of a classical boundary layer analysis may closely approximate the true physical situation. For this set of conditions, calculation of heat transfer and shear can be carried out in a consistent scheme accounting for the variation of the boundary layer edge conditions caused by the curved shock. The additional simplifying assumption of boundary layer similarity can be introduced when the analysis concerns the case of the highly-cooled wall. Indeed, for this case Lees[4] showed that the velocity gradient term in the transformed boundary layer equation may be neglected and the resulting equation is the Blasius equation for the flat plate. In reference 5, exactly this type of analysis is carried out to determine the conditions at the edge of the boundary layer. In the present report, the method is generalized and extended to include the quantitative effects of shock curvature on the laminar heat transfer.

Fluid particles having crossed the curved shock at different shock inclinations carry with them through the inviscid entropy layer different entropies and stagnation pressures. By identifying the streamline shock coordinate and the body coordinate corresponding to the point at which the streamline enters the boundary layer, the conditions at the boundary layer edge can be determined. Experimental evidence[6] shows that the static pressure on the conical surface of blunted cones is virtually constant at distances greater than 20 nose radii downstream of the shoulder and is equal to the sharp cone value. Use is made of this observation in the calculation of the boundary layer edge conditions.

The author takes this opportunity to thank Dr. V. Zakkay for suggesting this investigation and for his guidance in the work reported here.

METHOD OF ANALYSIS

The mass flow through the laminar boundary layer on an axisymmetric body at zero angle of attack is given by,

$$\dot{w} = 2\pi r \int_0^{\delta} \rho u dy' \tag{1}$$

introducing Lees variables,

$$\eta = \frac{\rho_e u_e r}{(2\tilde{S}_L)^{\frac{1}{2}}} \int_0^{y'} \frac{\rho}{\rho_e} dy' \tag{2}$$

$$\tilde{S}_L = \int_0^{s'} u_e \rho_e \mu_e r^2 ds' \tag{3}$$

(1) becomes

$$\dot{w} = 2\pi (2\tilde{S}_L)^{\frac{1}{2}} f(\eta_e) \tag{4}$$

considering streamtubes entering the shock at a distance y from the axis of symmetry (Fig. 1)

$$y^2 = \frac{2(2\tilde{S}_L)^{\frac{1}{2}} f(\eta_e)}{u_\infty \rho_\infty} \tag{5}$$

introducing the non-dimensional variable $\tilde{S}$ defined by

$$\tilde{S} = \frac{\tilde{S}_L}{u_\infty \rho_\infty \mu_\infty R_o^3} \tag{6}$$

the non-dimensional shock coordinate $\bar{y} \equiv \frac{y}{R_o}$ is given by

$$\bar{y} = \left[2^{3/2} f(\eta_e) R_{e\infty}^{-\frac{1}{2}} \tilde{S}^{\frac{1}{2}} \right]^{\frac{1}{2}} \tag{7}$$

where

$$R_{e\infty} \equiv \frac{u_\infty \rho_\infty R_o}{\mu_\infty}$$

defining the coefficient $a \equiv \left[2^{3/2} f(\eta_e) R_{e\infty}^{-\frac{1}{2}} \right]^{\frac{1}{2}}$ (8)

$$\bar{y} = a \tilde{S}^{1/4} \tag{9}$$

$$\left(\frac{\bar{y}}{a}\right)^4 = \tilde{S} = \int_0^{\bar{S}_s'} \bar{u}_e \bar{\rho}_e \bar{\mu}_e \bar{r}^2 d\bar{s} + \int_{\bar{S}_s'}^{\bar{S}'} \bar{u}_e \bar{\rho}_e \bar{\mu}_e \bar{r}^2 d\bar{s} \tag{10}$$

$$\left(\frac{\bar{y}}{a}\right)^4 = \int_0^{\bar{S}} \bar{u}_e\bar{\rho}_e\bar{\mu}_e\bar{r}^2 d\bar{s} - \int_0^{\cot\theta_B} \bar{u}_e\bar{\rho}_e\bar{\mu}_e\bar{r}^2 d\bar{s} + \int_0^{\bar{S}'_s} \bar{u}_e\bar{\rho}_e\bar{\mu}_e\bar{r}^2 d\bar{s}' \tag{11}$$

for $\bar{S} \geq \cot\theta_B$

$$\left(\frac{\bar{y}}{a}\right)^4 = \int_0^{\bar{S}} \bar{u}_e\bar{\rho}_e\bar{\mu}_e\bar{S}^2 \sin^2\theta_B d\bar{S} + A \tag{12}$$

For blunted cones of a given cone angle and freestream Mach number, the function $\bar{u}_e\bar{\rho}_e\bar{\mu}_e$ along the boundary layer edge is a function of the inclination of the shock. Assuming similar shock shapes for similar bodies and that the pressure on the conical portion of the body ($\bar{S} \geq \cot\theta_B$) is constant and equal to the sharp cone pressure, $\bar{u}_e\bar{\rho}_e\bar{\mu}_e$ is a function only of the non-dimensional shock coordinate $\bar{y}$.

$$\bar{u}_e\bar{\rho}_e\bar{\mu}_e = j(\bar{y}) \tag{13}$$

$$\frac{4\bar{y}^3}{a^4} = j(\bar{y})\sin^2\theta_B\bar{S}^2\frac{d\bar{S}}{d\bar{y}} \tag{14}$$

A technique for evaluating (14) graphically has been given by Rubin[7] to obtain the edge conditions as a function of $\bar{S}$. With the equation in this form, real gas effects may be computed by evaluating $j(\bar{y})$ using the real gas oblique shock relations and the real gas effects in the expansion to the inviscid cone surface. The following analysis assumes a perfect gas with $\gamma = 1.4$.

$$\frac{\bar{S}^3}{R_{e\infty}} = \frac{3}{2}\frac{1}{f^2(\eta_e)\sin^2\theta_B}\int_{\bar{y}_s}^{\bar{y}} \frac{\bar{y}^3}{j(\bar{y})}d\bar{y} + \frac{\cot^3\theta_B}{R_{e\infty}} \tag{15}$$

The first term on the right hand side of (15) is an exact form of the similarity parameter for the swallowing process. If the pressure distribution on the spherical cap is assumed to be a modified Newtonian and is used in computation of the value of $\bar{y}_s$, it is found that for $R_{e\infty} > 10,000$, the effects of $\bar{y}_s$ and $\frac{\cot^3\theta_B}{R_{e\infty}}$ are negligible for $\theta_B = 5°$ to $20°$. Thus, the form of the similarity parameter becomes,

$$\frac{\bar{S}^3}{R_{e\infty}} = \frac{3}{2}\frac{1}{f^2(\eta_e)\sin^2\theta_B}\int_0^{\bar{y}}\frac{\bar{y}^3}{j(\bar{y})}\,d\bar{y} \qquad (16)$$

or its equivalent forms $\bar{S}/R_{e\infty}^{1/3}$, $\bar{S}/R_{eos}^{1/4}$, where,

$$\frac{\bar{S}}{R_{eos}^{1/4}} = B^{1/4}\left[\frac{\bar{S}^3}{R_{e\infty}}\right]^{-1/4}$$

If Eq. (16) is integrated, the functional relationship between $\bar{S}$ and $\bar{y}$ is established and the conditions at the boundary layer edge are expressible directly as functions of the surface coordinate $\bar{S}$ or for general freestream conditions as functions of the similarity parameter $\bar{S}/R_{e\infty}^{1/3}$. The integration of (16) is performed numerically using the correlated shock shape of Ref. 8.

$$\bar{y} = 1.424\cos\theta_B\left[C_{DT}^{0.5}\left(\frac{\bar{x}}{\cos\theta_B}\right)\right]^{0.46}$$

where

$$C_{DT} = 2.0 - \cos^2\theta_B$$

The value of $\bar{y}$ where the shock takes the conical angle

$$\delta_c = \arcsin\left\{\frac{1}{M_\infty}\left[4.0 + 1.01(M_\infty\sin\theta_B - 3.43)\right]\right\}$$

is taken as the upper limit of integration $\bar{y}_c$ and is given by:

$$\bar{y}_c = \cos\theta_B\left\{.984C_{DT}\left[\frac{1}{\sin^2\delta_c} - 1\right]\right\}^{0.426}$$

Comparison of this shock shape with photographs of the shock show very good agreement with the actual shock in the region of interest $0 \le \bar{y} \le \bar{y}_c$.

The results of this computation expressing the boundary layer edge conditions as functions of the similarity parameter for several values of cone angles and freestream Mach numbers are given in Figs. 2 and 3.

For lower Reynolds number flow and for bodies of large nose blunting where the region $\bar{S} \approx \cot\theta_B$ is of interest, the similarity parameter $\bar{S}/R_{e\infty}^{1/3}$

breaks down. In this case, if the shock shape is known, Eq. (9) may be integrated from the stagnation point along the body with the streamline stagnation pressure determined by iteration from the previous point.

Having established the boundary layer edge conditions downstream of the shoulder to be functions of the parameter $\bar{S}/R_{e\infty}^{1/3}$, the assumption of similar boundary layer profiles enables the boundary layer properties $\bar{\delta}^*$, $\bar{\theta}$, $R_{e\theta}$ to be expressed in a general way, applicable to a family of blunted conical bodies. From the standard definitions, obtain,

$$\bar{\delta}^* = R_{e\infty}^{-\frac{1}{2}}(2\tilde{S})^{\frac{1}{2}}\frac{1}{\bar{\rho}_e\bar{u}_e\bar{r}}\frac{\gamma-1}{2}M_e\int_0^\infty[f'-(f')^2]d\eta \tag{18}$$

$$\bar{\theta} = R_{e\infty}^{-\frac{1}{2}}(2\tilde{S})^{\frac{1}{2}}\frac{1}{\bar{\rho}_e\bar{u}_e\bar{r}}\int_0^\infty[f'-(f')^2]d\eta \tag{19}$$

$$R_{e\infty} = R_{e\infty}^{\frac{1}{2}}\frac{(2\tilde{S})^{\frac{1}{2}}}{\bar{r}\bar{\mu}_e}\int_0^\infty[f'-(f')^2]d\eta \tag{20}$$

From (18), (19) and (20) it can be established that the boundary layer parameters $\bar{\delta}^*R_{e\infty}^{1/3}$, $\bar{\theta}R_{e\infty}^{1/3}$, $R_{e\theta}R_{e\infty}^{-2/3}$ are functions of the similarity parameter $\bar{S}/R_{e\infty}^{1/3}$. The results of numerical calculations expressing these parameters as functions of the similarity parameter for several values of freestream Mach numbers for a cone of half angle 15° are given in Figs. 4, 5 and 6. The effect of blunting on $R_{e\theta}$ at different $R_{e\infty}$ is shown in Figs. 7 and 8.

At hypersonic speeds, where effects of the external stream gradients on stability are as yet uncertain, the knowledge of R_{ex} or $R_{e\theta}$ alone along the body surface may not be enough to predict the onset of transition. As pointed out most recently by Stetson and Rushton[9], when transition appears on the body between the shoulder and the swallowing distance, $R_{e\theta T}$ will vary from a blunt body value of approximately 340 to a conical body value of approximately 700. From shock tunnel experiments[9] conical transition

will occur when $R_{e\theta} < 340$ at $S \geq .3S_c$ and blunt body transition will occur when $R_{e\theta} > 340$ at $S_c \leq .03S$.

With the generality afforded by the results in Fig. 6, the range of $R_{e\infty}$ for which conical and blunt body transition will occur can be found as a function of unit freestream Reynolds number and degree of blunting. The results are given in Figs. 8a and 8b, for the specific family of 8° blunted cones at $M_\infty = 5.5$. The extension of these results to include the effects of cone angle and Mach number must necessarily await additional experimental transition data at different Mach numbers and cone angles.

Fig. 8b indicates that the effects of bluntness on transition are very important in the design of hypersonic flight vehicles. For example, at Mach 5.5 and $\theta_B = 8°$ at 100,000 ft., a vehicle with a three inch nose radius will undergo transition at some point along the surface between 4.6 ft. and 20.8 ft., corresponding to $R_{e\theta}$ of 340 and 680 respectively. Therefore, the assumption of one type of transition for a body having a surface length of between 4 and 20 ft. can result in error over a large part of the conical surface.

Nagamatsu et al[12] report transition on a blunted cone of .2 in. radius 5° cone half angle, $M_\infty = 11$ with the stagnation conditions, $T_o = 1400°K$, $P_o = 1300$ psia. Transition is observed to occur at a distance of 18.72 in. from the cone tip. With the same conditions but at $P_o = 890$ psia, no transition is observed within the distance of 45.38 inches. Determination of the $R_{e\theta}$ for these conditions indicates that at $P_o = 890$ $R_{e\theta}$ is below 700 for the entire length and since the flow is laminar, it may be assumed that these conditions are in the conical transition region. At 1300 psia, $R_{e\theta}$ is about 340 at 18.72 in from the tip, where transition is observed. These calculations lead to the conclusion that in going from $R_{e\infty} = .8 \times 10^4$ to $R_{e\infty} = .13 \times 10^5$, the transition moves from conical to blunt body type. This suggests, moreover, that the influence of Mach number and cone angle on the type of transition is significant.

By assuming a linear Mach number variation along the conical surface, Zakkay and Krause[5] obtained the expression:

$$\bar{S}_c = \left[\frac{3}{2}\frac{(R/\gamma)^{\frac{1}{2}}\rho_\infty^2 u_\infty^2}{\lambda P_c}\frac{(3M_c+M_s)}{f^2(\eta_e)\sin^2\theta_B}\frac{\bar{y}_c^4 R_o}{}\right]^{1/3} \tag{21}$$

for the extent of the bluntness effects (i.e. the swallowing distance). Cast in the form of the present analysis, this expression is:

$$\frac{\bar{S}_c}{R_{e\infty}^{1/3}} = \left[\frac{1.5M_\infty \bar{y}_c^4}{\frac{P_c}{P_\infty} f^2(\eta_e)\sin^2\theta_B (3M_c+M_s)}\right]^{1/3} \tag{22}$$

or dimensionally as

$$\frac{P_\infty^{1/3} S_c}{R_o^{4/3}(\rho_\infty u_\infty)^{2/3}} = \left[\frac{3}{2}(R/\gamma)^{\frac{1}{2}}\frac{P_\infty}{P_c}\frac{\bar{y}_c^4}{\lambda(3M_c+M_s)f^2(\eta_e)\sin^2\theta_B}\right]^{1/3} \tag{23}$$

Eq. (21) or (22) can be used to conveniently express the swallowing distance as a function of the degree of blunting and freestream conditions. The results for several cone angles are given in Fig. 9 in comparison with the swallowing distance computed by numerically integrating (16) to the upper limit $\bar{y}_c$. Where $\bar{y}_c$ is defined as the non-dimensional shock coordinate at which the shock is nearly conical. Specifically, Ref. 9, uses the value of $\bar{y}_c$ where the shock angle yields a Mach number on the inviscid cone of .95 M_c. An examination of the integrand of (16) indicates that the value of $\bar{S}_c/R_{e\infty}^{1/3}$ is strongly dependent on the value of $\bar{y}_c$. The critical nature of the value of $\bar{y}_c$ is evident in the approximate form of the swallowing distance parameter given by Eq. (22) where $\bar{y}_c$ appears as the fourth power relative to the other terms in the expression. Physically this expresses the fact that most of the flow in the boundary layer near the swallowing point has entered the shock at values of $\bar{y}$ near $\bar{y}_c$. This implies that the shape of the shock in the $\bar{y}_c$ region is more important than the shape

of the shock at smaller values of $\bar{y}$, for the determination of $\bar{S}_c$. Thus, if the shock is assumed to have the constant conical angle throughout (M_s replaced by M_c in Eq. 22), and the correct value of $\bar{y}_c$ from the curved shock retained, the approximate Eq. 22 simplifies to:

$$\frac{\bar{S}_c}{R_{e\infty}^{1/3}} = \left[\frac{1.5\bar{y}_c^4 M_\infty}{P_c/P_\infty f^2(\eta_e)\sin^2\theta_B(4M_c)}\right]^{1/3} \tag{24}$$

the results shown on Fig. 9 indicate that Eq. (24) approximates the shock shape more closely in the region near $\bar{y}_c$ than does Eq. (22) (since the Mach number will approach M_c asymptotically, as shown in Fig. 2). The importance of approximating the shock shape near $\bar{y}_c$ rather than an overall approximation is shown in Fig. 9 where the approximation (22) is seen to be in closer agreement with the numerical integration. The role of the shock shape in the region near $\bar{y}_c$ in the calculation of $\bar{S}_c$ lies at the root of the descrepancy between the results of this method and the momentum integral method of Wilson[10,11].

HEAT TRANSFER

The variation of the heat transfer along the conical portion of the body is due to the local surface coordinate and the external stream conditions at the boundary layer edge affecting the physical plane temperature gradient at the wall. The effect of the external stream vorticity on the boundary layer profile is assumed to be negligible due to the Reynolds numbers to which the present analysis is applied. The heat transfer is calculated in the non-dimensional form $Nu/(R_{eol})^{\frac{1}{2}}$ where the Nusselt number and the Reynolds number are defined with respect to the normal shock stagnation conditions.

$$Nu = \frac{C_{poe} R_o q_w}{k_{oe}(h_{oe} - h_{ow})} \tag{25}$$

$$R_{eol} = \frac{(h_{oe})^{\frac{1}{2}} \rho_{ol} R_o}{\mu_{oe}} \tag{26}$$

The heat transfer parameter $Nu/(R_{eol})^{\frac{1}{2}}$ in terms of the analysis becomes,

$$Nu/(R_{eol})^{\frac{1}{2}} = .333 D \bar{P}_r^{1/3} \frac{\bar{u}_e \bar{\rho}_e \bar{\mu}_e \bar{r}}{\bar{S}^{\frac{1}{2}}} \tag{27}$$

where

$$D = \left[\frac{u_\infty \rho_\infty \mu_\infty}{(h_{ol})^{\frac{1}{2}} \rho_{ol} \mu_{ol}} \right]^{\frac{1}{2}}$$

and $\bar{P}_r$ is an average Prandtl number across the boundary layer. In obtaining the form of Eq. (24), the conclusion of Lees[4] for the cold wall

$$\frac{g_w'}{1-g_w} \simeq .47 \bar{P}_r^{1/3}$$

is used.

The results of the numerical evaluation of (25) for a cone of 15° half angle at freestream Mach number of 20, is presented in Fig. 10. Shown also, are the limiting values obtained by assuming normal shock and conical shock conditions to exist at the boundary layer edge.

The influence of shock curvature on heat transfer as illustrated in Fig. 10 for conditions of $M_\infty = 20$, $R_{e\infty}$(per ft.) $= 1.0 \times 10^5$ is representative of the quantitative influence of shock curvature on the heat transfer to the portion of the body downstream of the shoulder.

Examining the variable terms appearing on the right hand side of (25)

$$\bar{u}_e \bar{\rho}_e \bar{\mu}_e = f_1 (\bar{s}/R_{e\infty}^{1/3})$$

$$\bar{r} = R_{e\infty}^{1/3} (\bar{s}/R_{e\infty}^{1/3}) \sin\theta_B$$

$$\tilde{S}^{\frac{1}{2}} = \frac{R_{e\infty}^{\frac{1}{2}}}{2^{3/2} f(\eta_e)} \bar{y} (\bar{s}/R_{e\infty}^{1/3})$$

Eq. (25) is seen to have the form,

$$\frac{Nu}{(R_{eo})^{\frac{1}{2}}} = R_{e\infty}^{-1/6} F_1 (\bar{s}'/R_{e\infty}^{1/3}) \qquad (28)$$

where

$$F_1 (\bar{s}'/R_{e\infty}) = .333 \bar{D} \bar{P}_r^{1/3} \sin\theta_B 2^{3/2} f(\eta_e) \frac{\bar{s}'}{R_{e\infty}^{1/3}} \frac{f_1 (\bar{s}'/R_{e\infty}^{1/3})}{\bar{y} (\bar{s}'/R_{e\infty}^{1/3})}$$

Thus, the heat transfer parameter $Nu/(R_{eo})^{1/3}$ is a function of the similarity parameter $\bar{s}/R_{e\infty}^{1/3}$ and by Eq. (17) also of the similarity parameter $\bar{s}/R_{eos}^{1/4}$. The value of $Nu/(R_{eo1})^{1/3}$ as a function of $\bar{s}/R_{e\infty}^{1/3}$ represents the effect of the shock curvature on the laminar heat transfer along the conical surface for a family of blunted cones. The heat transfer calculations for a family of cones at various values of the freestream Mach number are presented in Fig. 12.

Calculation of the heat transfer on the conical part of the body based on constant external stream stagnation properties corresponding to normal shock or conical shock conditions can be made in the cases of high $R_{e\infty}$ or low $R_{e\infty}$ or respectively. Essentially, if the surface coordinate is small with respect to the swallowing distance (high $R_{e\infty}$), normal shock stagnation con-

ditions will exist at the boundary layer edge and similarly, if the surface coordinate is large with respect to the swallowing distance, conical shock stagnation conditions may be assumed to prevail. It follows, that bluntness effects will be important when the surface coordinate is on the same order as the swallowing distance and in these cases, the heat transfer should be calculated by accounting for the variation in external stream properties. The typical heat transfer results accounting for bluntness effects, is shown in Fig. 10 with respect to the limits of normal and c nical shock stagnation conditions. Qualitatively, Fig. 10 indicates that the choice of nose radius will influence downstream heat transfer at sections whose position with respect to the swallowing distance is shifted from $> .5s_c$ to $< .5s_c$ as nose radius is increased. These conditions are approximated in the conditions of Fig. 11 where the results of downstream heat transfer are shown as the result of an increase in nose radius from 1.2 to 3 inches.

The laminar heat transfer results must of course be accepted only when transition can be assumed to occur downstream. In light of the previous discussion of transition for the case of the condition of Fig. 8, when a rough extrapolation of results is assumed valid*, conical transition may be expected to prevail in both cases, and transition will occur downstream of the region indicated.

---

*And this is by no means apparent - as indicated, more transition data at different M_∞ and θ_B must be accumulated before Fig. 8a can be generalized for M_∞ and θ_B.

RESULTS AND CONCLUSIONS

The general boundary layer parameters δ^*, θ, $R_{e\theta}$, $Nu/(R_{ecl})^{\frac{1}{2}}$ are found and presented for a family of correlated cones and shock shapes at Mach numbers from 5 to 20, for distances along the conical surface corresponding to the swallowing distance. The effects of nose bluntness on transition and heat transfer are judged in terms of the swallowing distance, for which a simplified approximation is presented (Eq. 24). Based on the general $R_{e\theta}$ results along the conical surface, regions of $R_{e\infty}$ for which conical transition ($R_{e\theta T} \approx 700$) and blunt body transition ($R_{e\theta T} = 340$) can be expected is presented in Fig. 8a. For family of 8° cones at $M_\infty = 5.5$ the reversal region will occur for $.216 \times 10^5 < R_{e\infty} < .26 \times 10^6$. The need for additional experimental studies to extend the results to account for M_∞ and cone angle effects on transition is indicated. The investigation of heat transfer accounting for shock curvature effects shows that the laminar heat transfer to the conical part of the body can be influenced by the degree of nose blunting when the nose radius is increased enough to shift that part of the body from $> .5s_c$ to $< .5s_c$.

REFERENCES

1. Ferri, A. and Libby, P. A., "Note on an Interaction between the Boundary Layer and the Inviscid Flow," J. Aero. Sci., 21, 2, P. 130, February 1954.
2. Ferri, A., "Some Heat Transfer Problems in Hypersonic Flow," Reprinted from Aeronautics and Astronautics, Pergamon Press, New York, pp. 344-377, 1960.
3. Ferri, A., Zakkay, V. and Ting, L., "Blunt Body Heat Transfer at Hypersonic Speed and Low Reynolds Numbers," Polytechnic Institute of Brooklyn PIBAL Report No. 611, June 1960.
4. Lees, L., "Laminar Heat Transfer over Blunt-Nosed Bodies at Hypersonic Flight Speeds," Jet Prop., Vol. 26, No. 4, pp. 259-269, April 1956.
5. Zakkay, V. and Krause, E., "Boundary Conditions at the Outer Edge of the Boundary Layer on Blunted Conical Bodies," AIAA Journal, Vol. 1, No. 7, pp. 1671-1672, 1963.
6. Burke, A. F. and Curtis, James T., "Blunt-Cone Pressure Distributions at Hypersonic Mach Numbers," J. Aerospace Sci., Vol. 29, 1962, pp. 237-238.
7. Rubin, I., "Shock Curvature Effect on the Outer Edge Conditions of a Laminar Boundary Layer," AIAA Journal, 1, pp. 2850-2852, 1963.
8. Klaimon, J. H., "Bow Shock Correlation for Slightly Blunted Cones," J. Aero. Sci., Vol. 1, No. 2, February 1963.
9. Stetson, K. F. and Rushton, G. H., "A Shock Tunnel Investigation of the Effects of Nose Bluntness, Angle of Attack and Boundary Layer Cooling on Boundary Layer Transition at a Mach Number of 5.5," AIAA Paper No. 66-495, June 1966.
10. Wilson, R. E., "Laminar Boundary - Layer Growth on Slightly - Blunted Cones at Hypersonic Speeds," J. Spacecraft and Rockets, 2, pp. 490-496, 1965.
11. Wilson, R. E., "Laminar and Turbulent Boundary Layers on Slightly-Blunted Cones at Hypersonic Speeds," NOLTR 66-54, 1966.

12. Nagamatsu, H. T., Graber, B. C. and Sheer, R. E., "Roughness, Bluntness, and Angle-of-Attack Effects on Hypersonic Boundary Layer Transition," (1966), J. Fluid Mechanics, Vol. 24.

13. Sims, J. L., "Tables of Supersonic Flow around Right Circular Cones at Zero Angle of Attack," 1964, NASA SP-3004.

14. Minzner, R. A., Champion, K. S. W., Pond, H. L., "The ARDS Model Atmosphere," 1959, Air Force Cambridge Research Center, TR-59-267, August 1959.

15. Reinecke, W. G., "Charts for Use with Hypersonic Air Wind Tunnels," (1964) ARL 64-56.

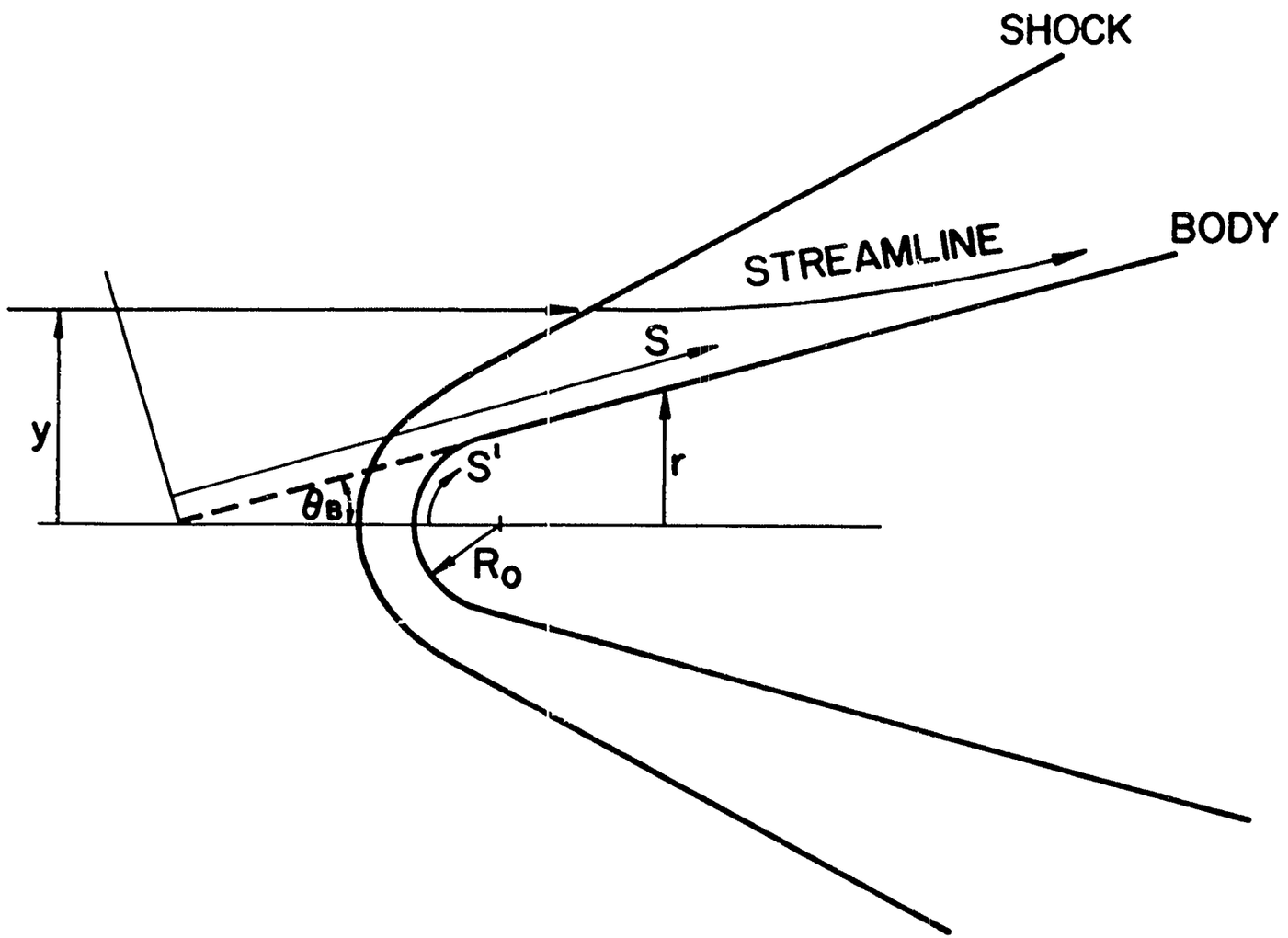

FIG. 1 BODY-SHOCK GEOMETRY AND COORDINATE SYSTEM

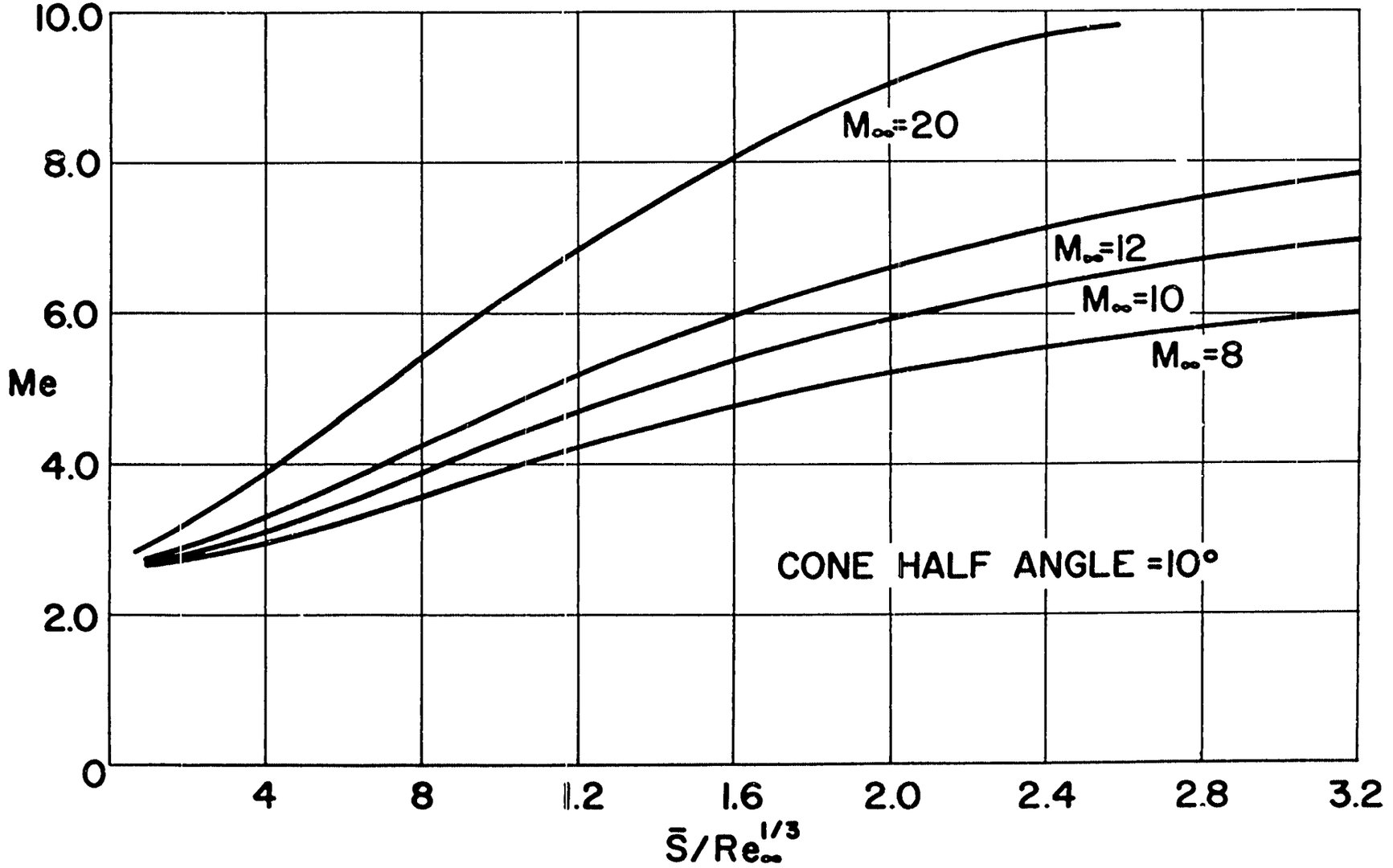

FIG. 2 MACH NUMBER DISTRIBUTION (M_e vs. SIMILARITY PARAMETER $\bar{S}/R_{e\infty}^{1/3}$)

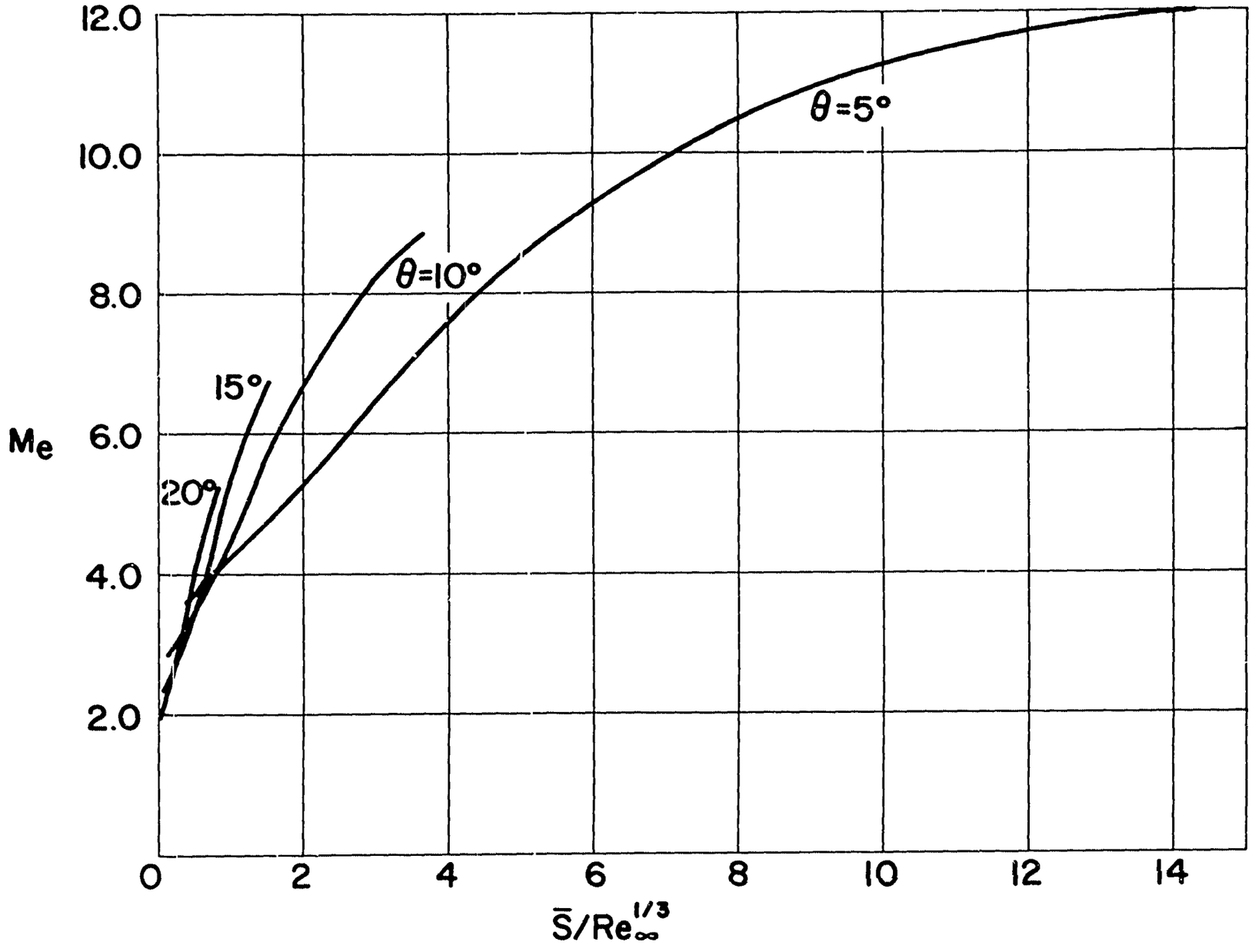

FIG. 3 MACH NUMBER DISTRIBUTION (M_e vs. SIMILARITY PARAMETER $\bar{S}/R_{e\infty}^{1/3}$), M_∞ = 15

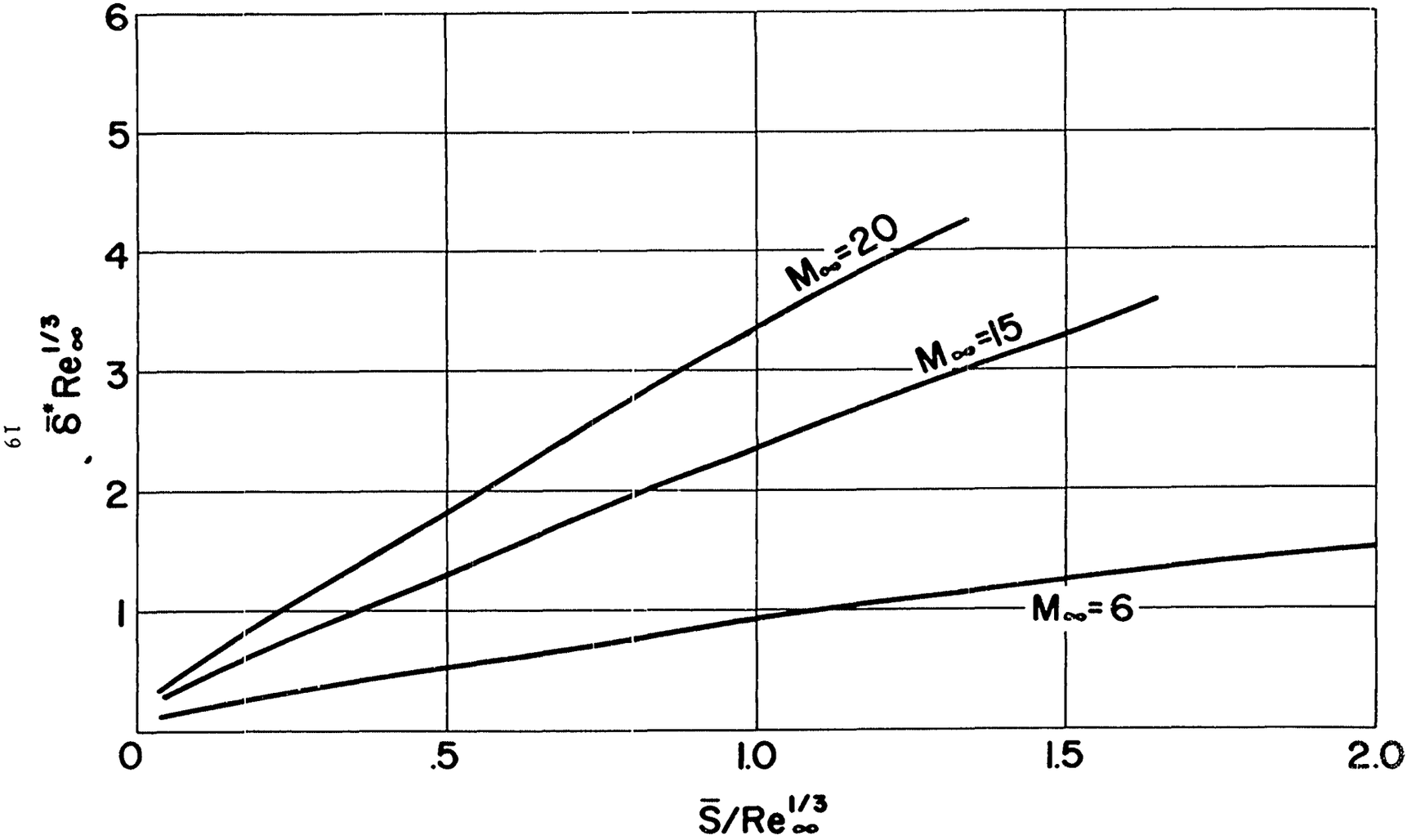

FIG. 4 DISPLACEMENT THICKNESS PARAMETER $\bar{\delta}^* R_{e\infty}^{1/3}$ AS A FUNCTION OF THE SIMILARITY PARAMETER $\bar{S}/R_{e\infty}^{1/3}$, 15° CONE HALF ANGLE

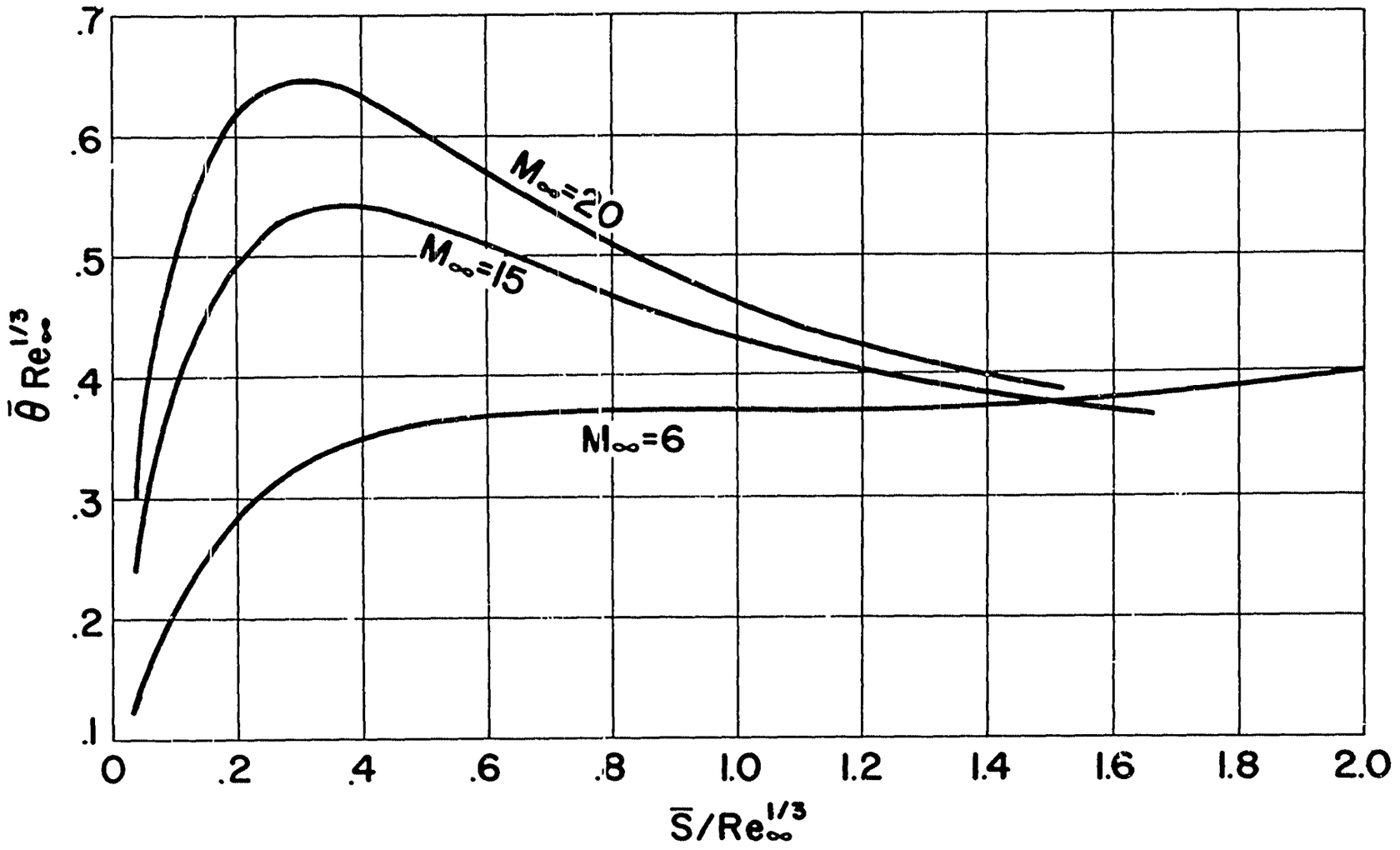

FIG. 5 MOMENTUM THICKNESS PARAMETER $\bar{\theta}R_{e\infty}^{1/3}$ AS A FUNCTION OF THE SIMILARITY PARAMETER $\bar{S}/R_{e\infty}^{1/3}$. 15° CONE HALF ANGLE

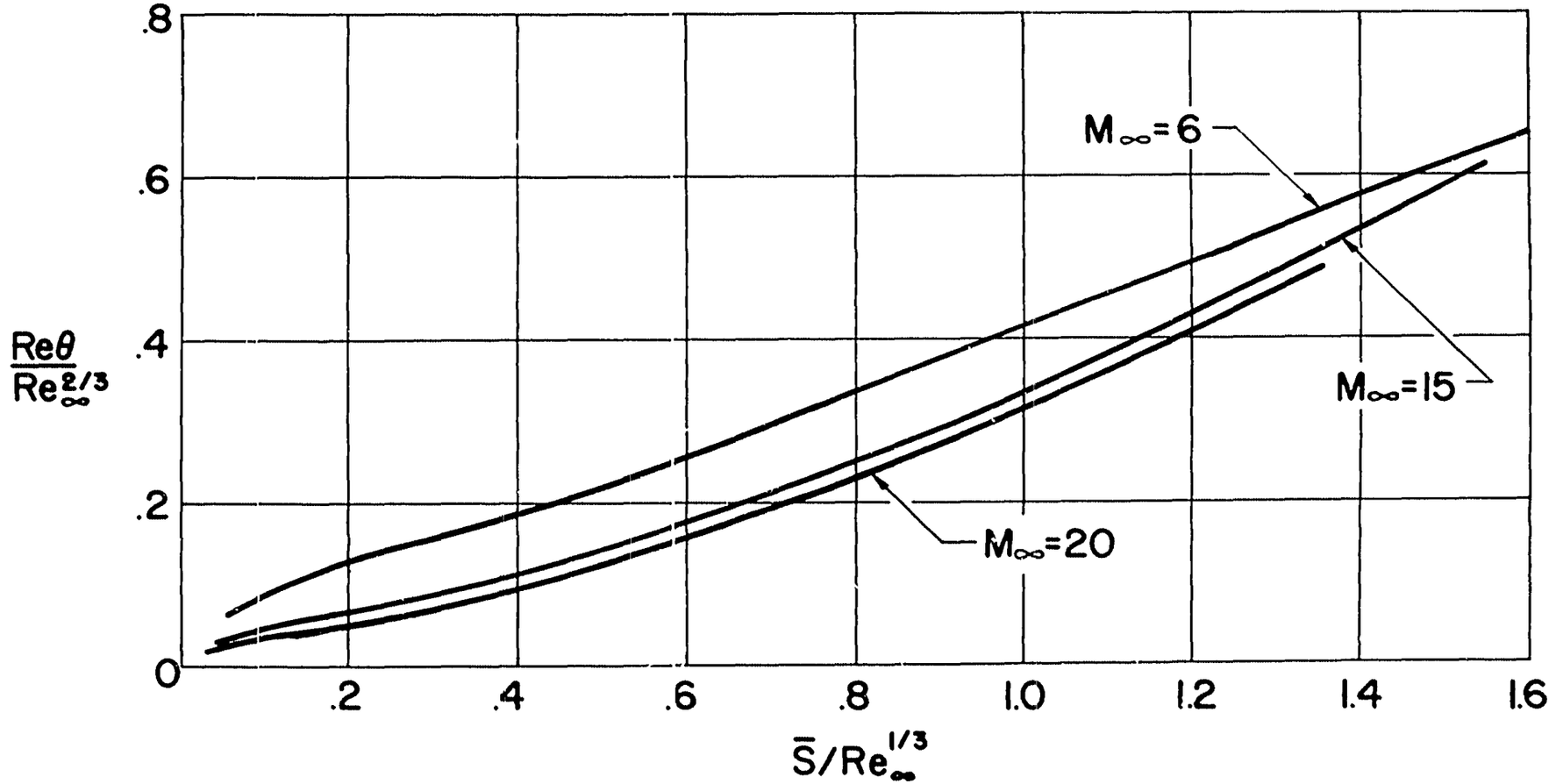

FIG. 6 MOMENTUM THICKNESS REYNOLDS NUMBER PARAMETER $R_{e\theta}/R_{e\infty}^{2/3}$ AS A FUNCTION OF THE SIMILARITY PARAMETER $\bar{S}/R_{e\infty}^{1/3}$, 15° CONE HALF ANGLE

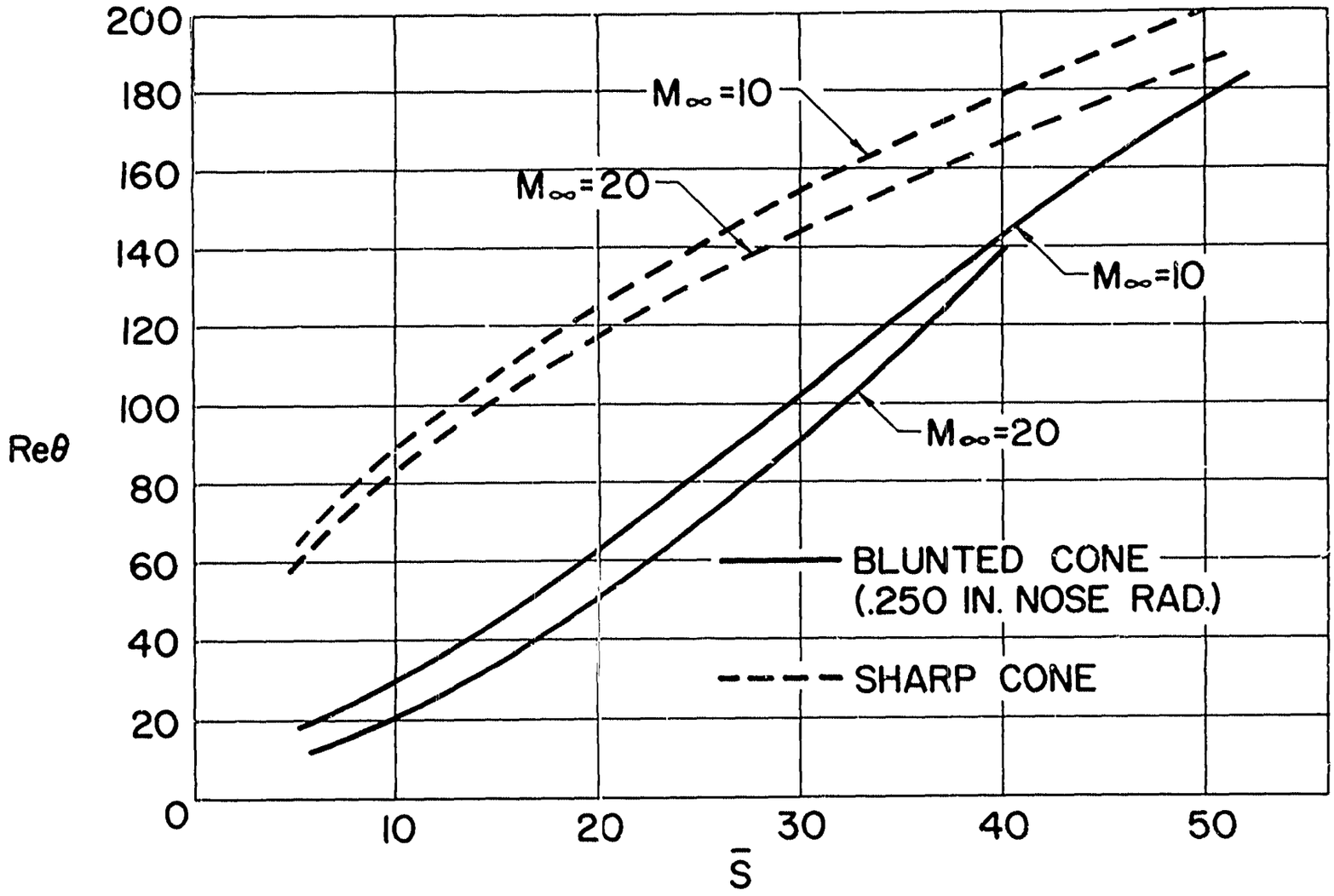

FIG. 7a MOMENTUM THICKNESS REYNOLDS NUMBER ($R_{e\theta}$) DISTRIBUTION FOR BLUNT AND SHARP 10° HALF ANGLE CONE ($R_{e\theta}$ vs. $\bar{S}$), UNIT FREESTREAM REYNOLDS NUMBER = 10^5

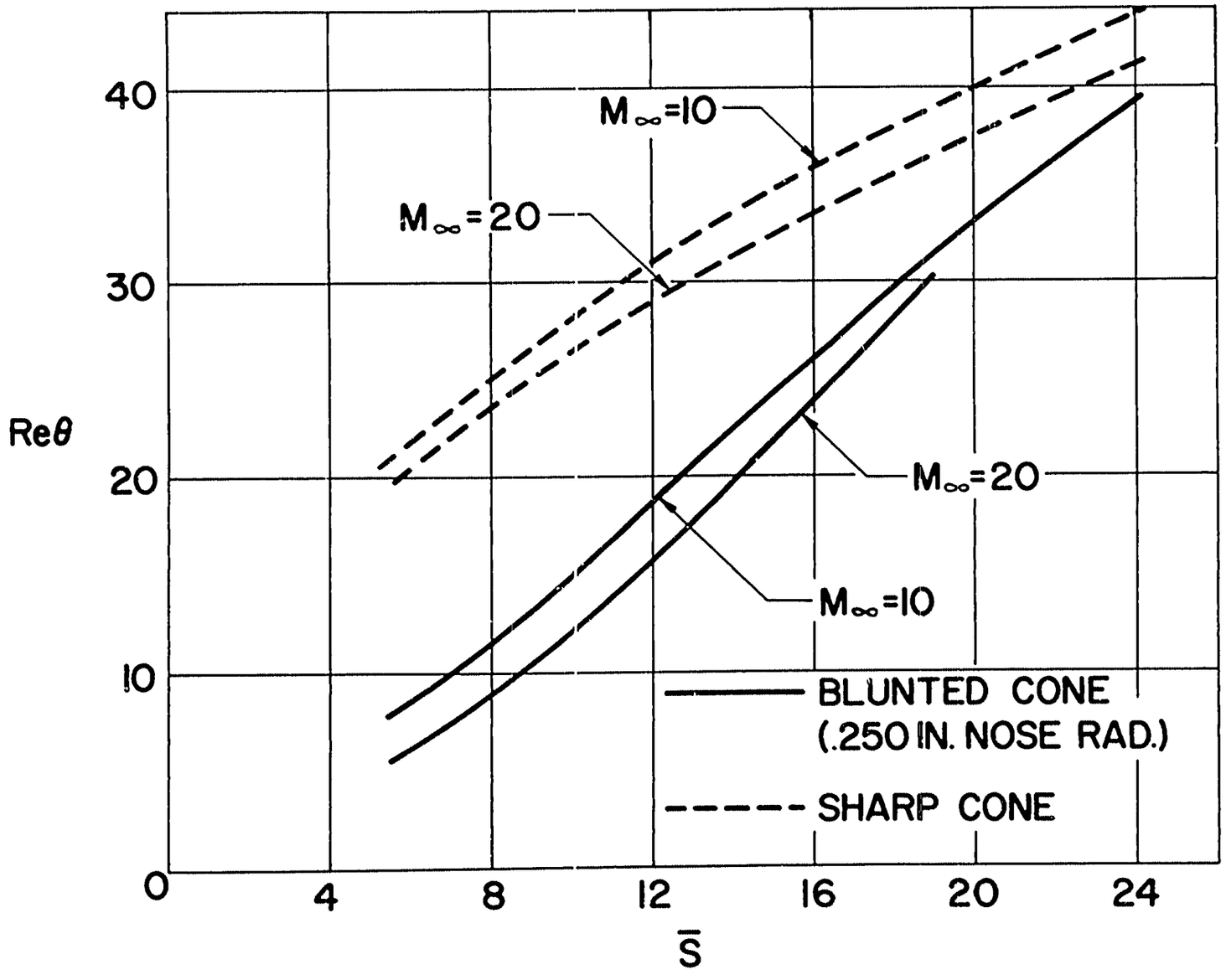

FIG. 7b MOMENTUM THICKNESS REYNOLDS NUMBER ($R_{e\theta}$) DISTRIBUTION FOR BLUNT AND SHARP 10° HALF ANGLE CONE ($R_{e\theta}$ vs. $\bar{S}$), UNIT FREESTREAM REYNOLDS NUMBER = 10^4

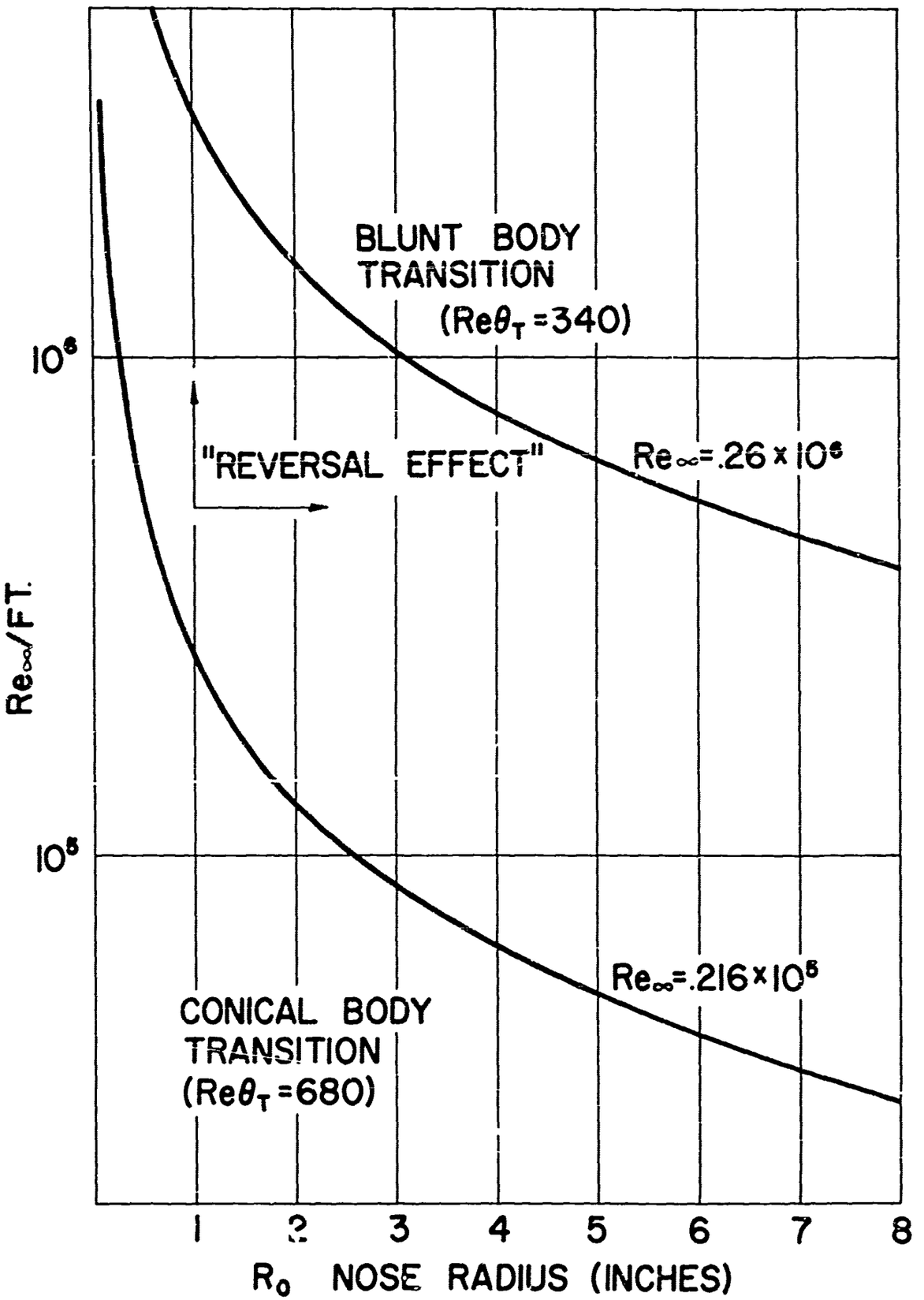

FIG. 8a REGIONS OF CONICAL AND BLUNT BODY TRANSITION IN TERMS OF UNIT FREESTREAM REYNOLDS NUMBER AND NOSE RADIUS, M_∞ = 8, CONE HALF ANGLE (θ_B) = 5.5°

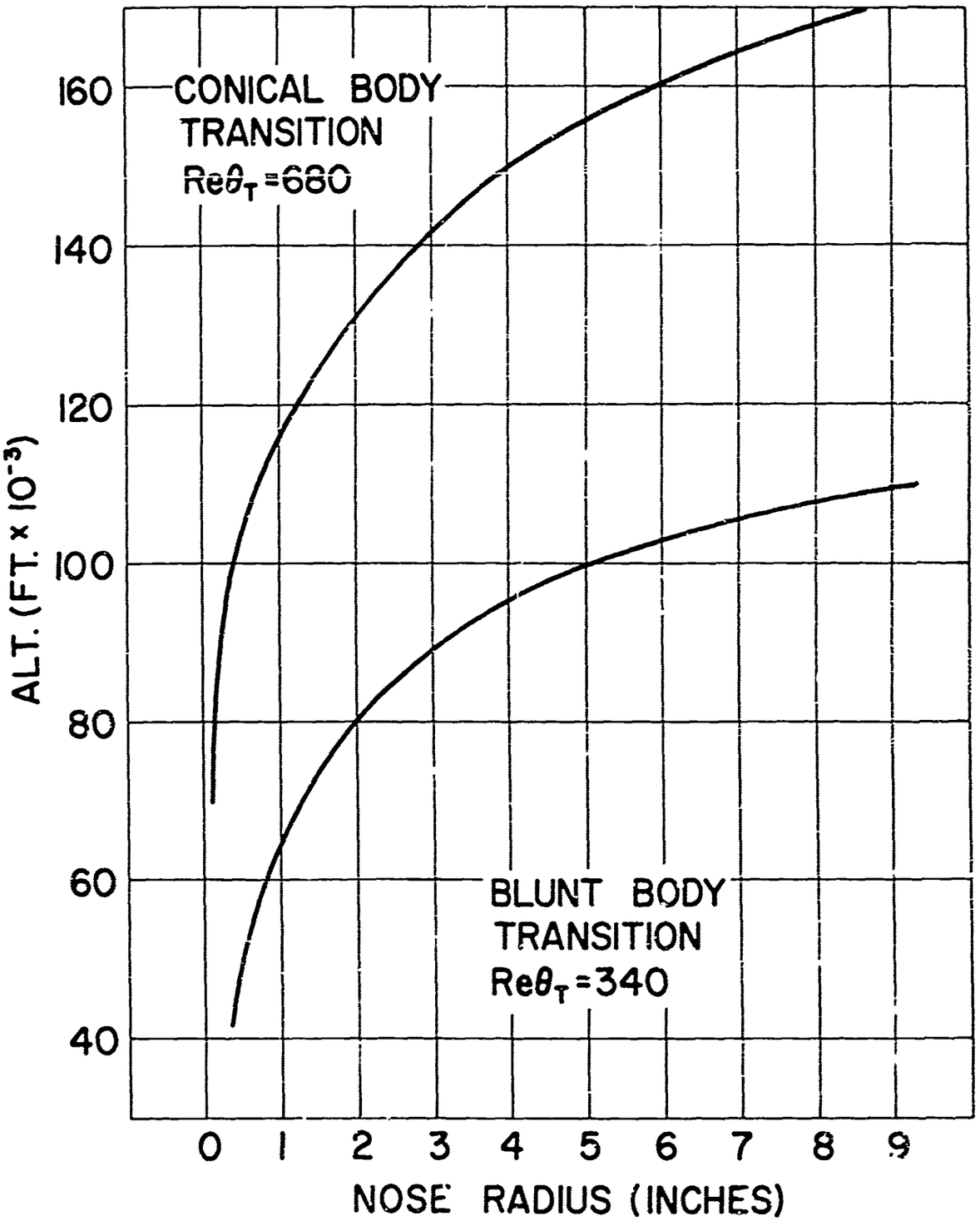

FIG. 8b REGIONS OF CONICAL AND BLUNT BODY TRANSITION IN TERMS OF FLIGHT ALTITUDE AND NOSE RADIUS, $M_\infty = 8$, CONE HALF ANGLE (θ_B) = 5.5°

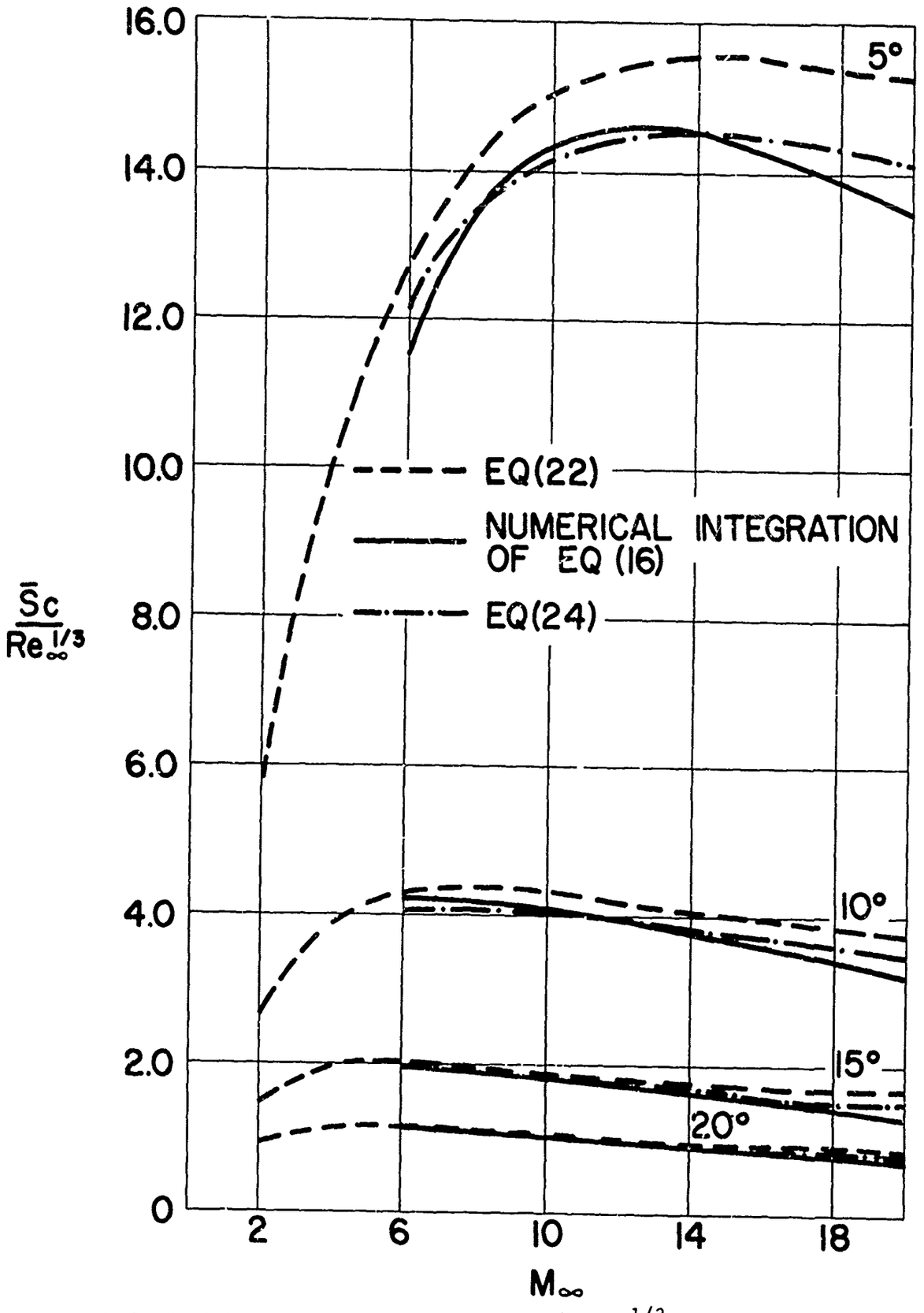

FIG. 9 SWALLOWING DISTANCE PARAMETER $\bar{S}_c/R_{e\infty}^{1/3}$ AS A FUNCTION OF FREESTREAM MACH NUMBER, ($\bar{S}_c/R_{e\infty}^{1/3}$ vs. M_∞)

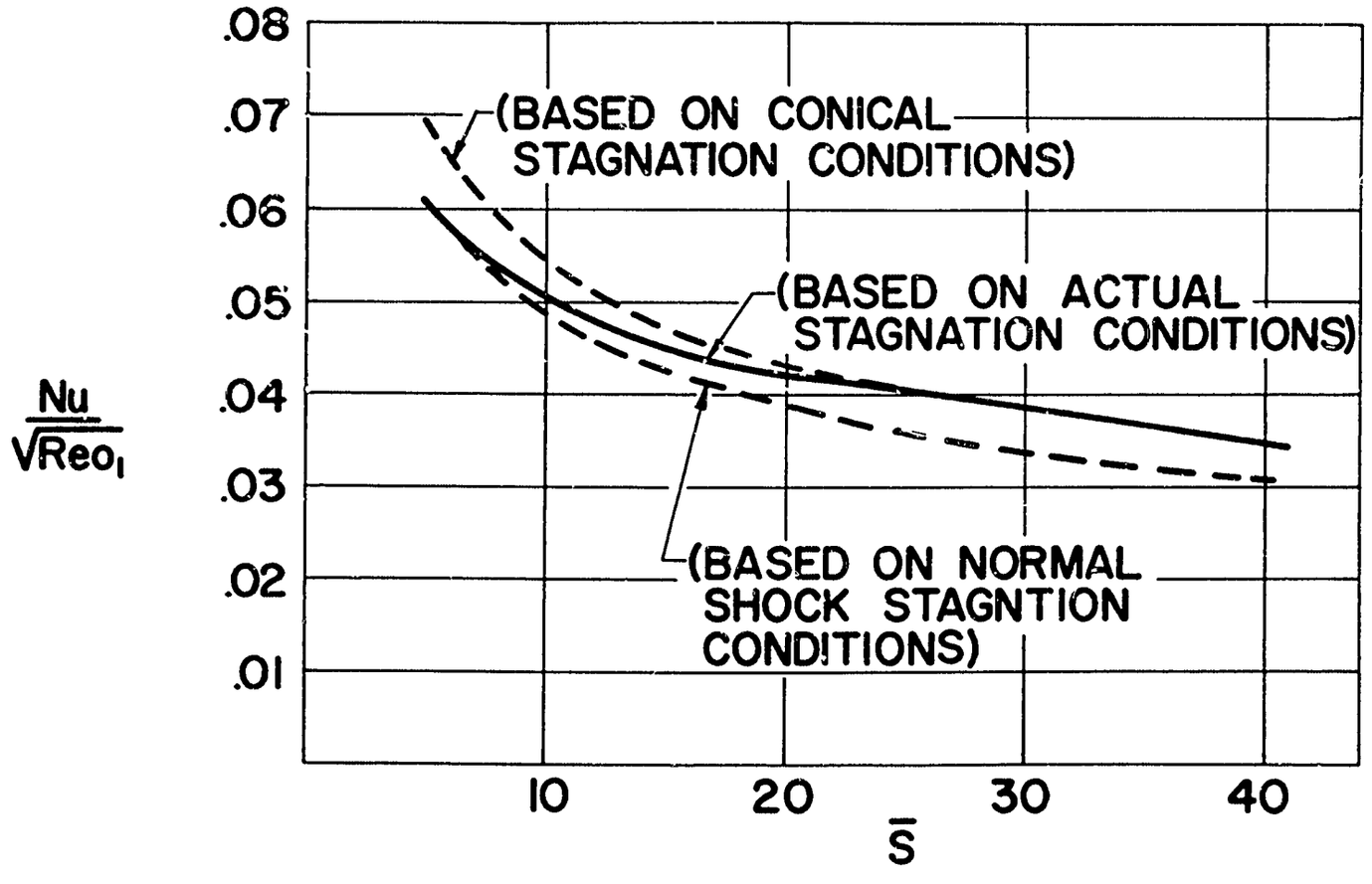

FIG. 10 HEAT TRANSFER DISTRIBUTION $(Nu/(R_{eo1})^{\frac{1}{2}}$ vs. $\bar{S})$, $M_\infty = 20$, $\theta_B = 10°$, UNIT FREESTREAM REYNOLDS NUMBER = 10^5

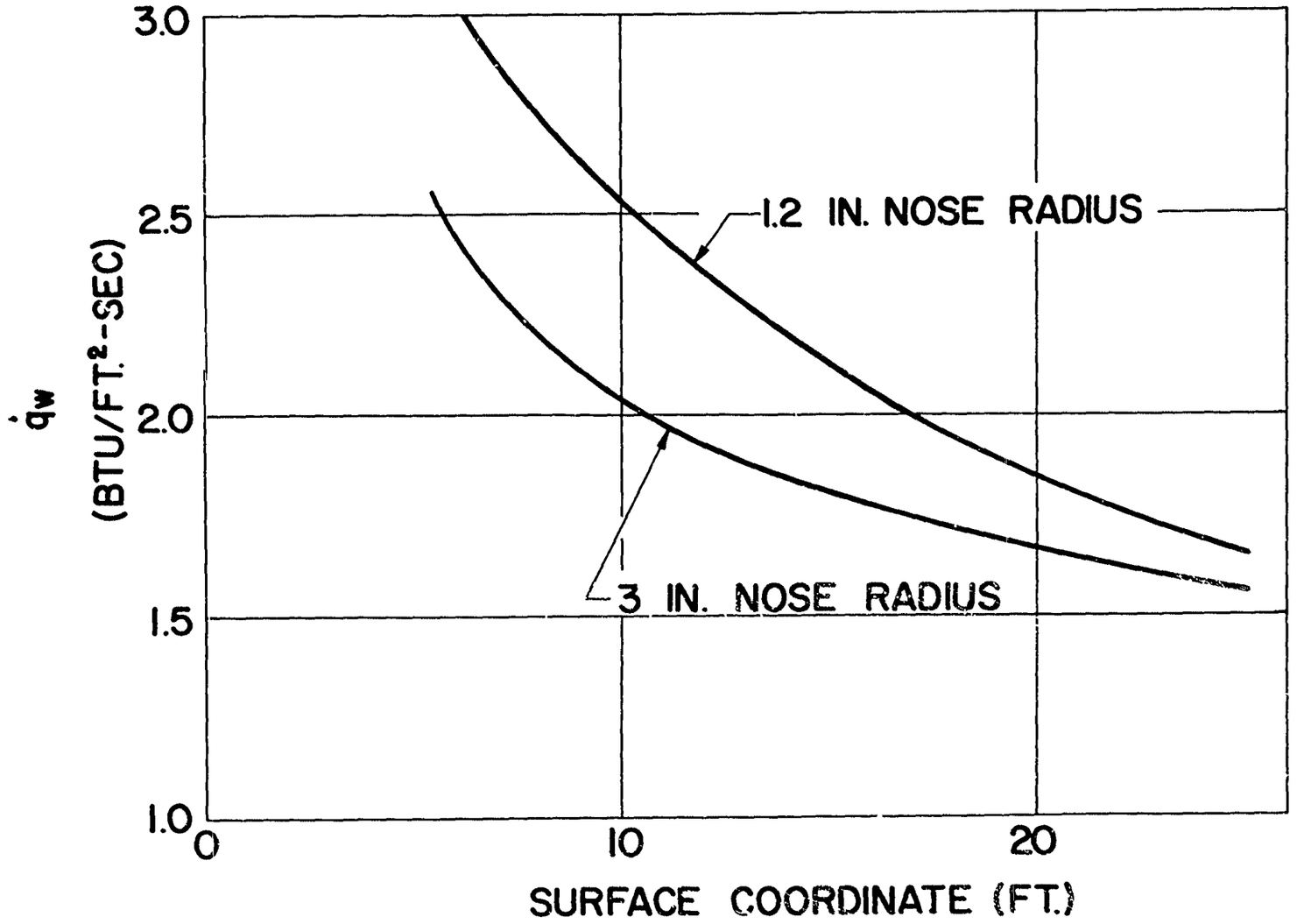

FIG. 11 EFFECTS OF NOSE RADIUS ON DOWNSTREAM HEAT TRANSFER ($\dot{q}_w$ vs. s), M_∞= 10, θ_B = 5° UNIT FREESTREAM REYNOLDS NUMBER = 0.73×10^5

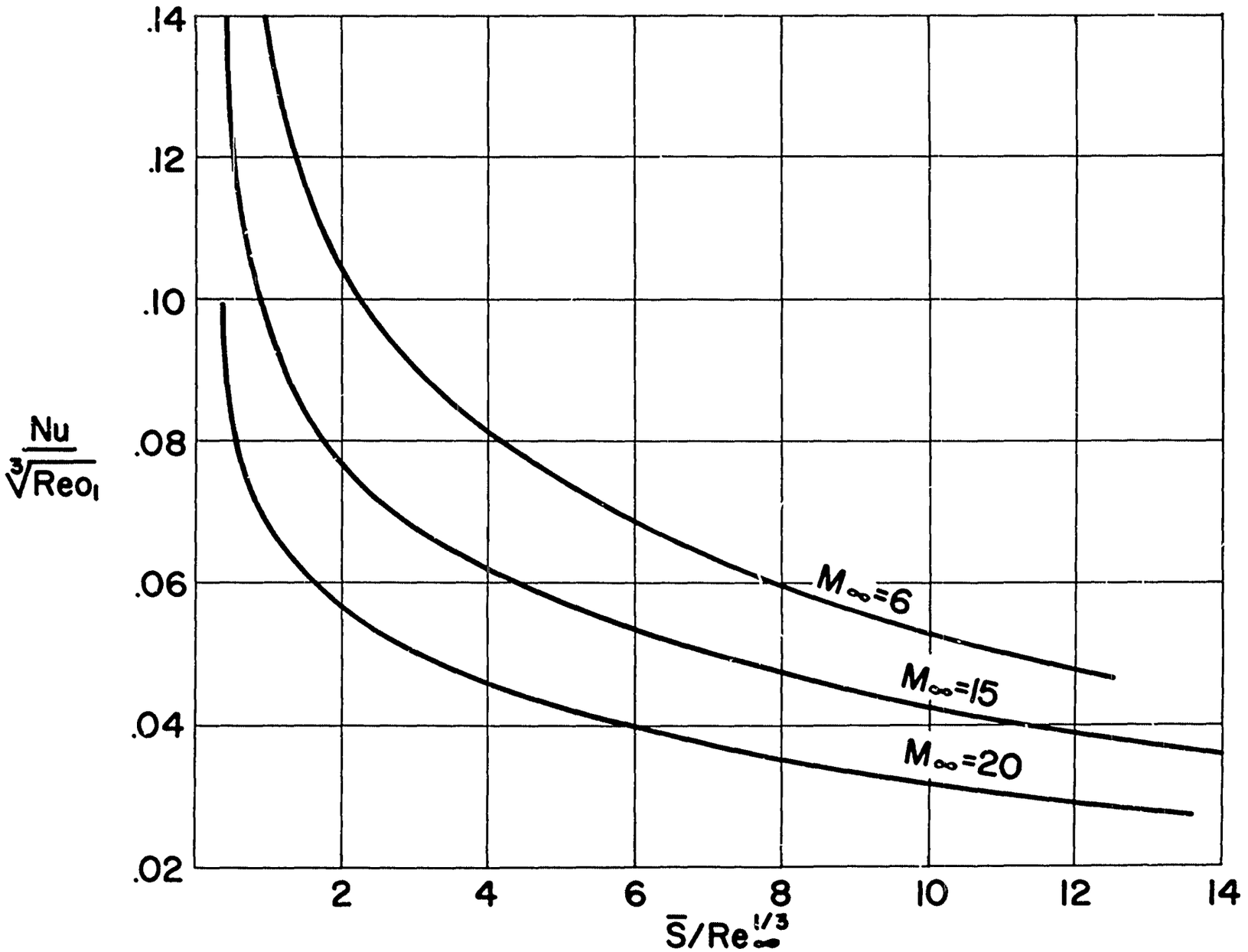

FIG. 12a HEAT TRANSFER PARAMETER $Nu/(R_{eo1})^{1/3}$ AS A FUNCTION OF THE SIMILARITY PARAMETER $\bar{S}/R_{e\infty}^{1/3}$, $\theta_B = 5°$

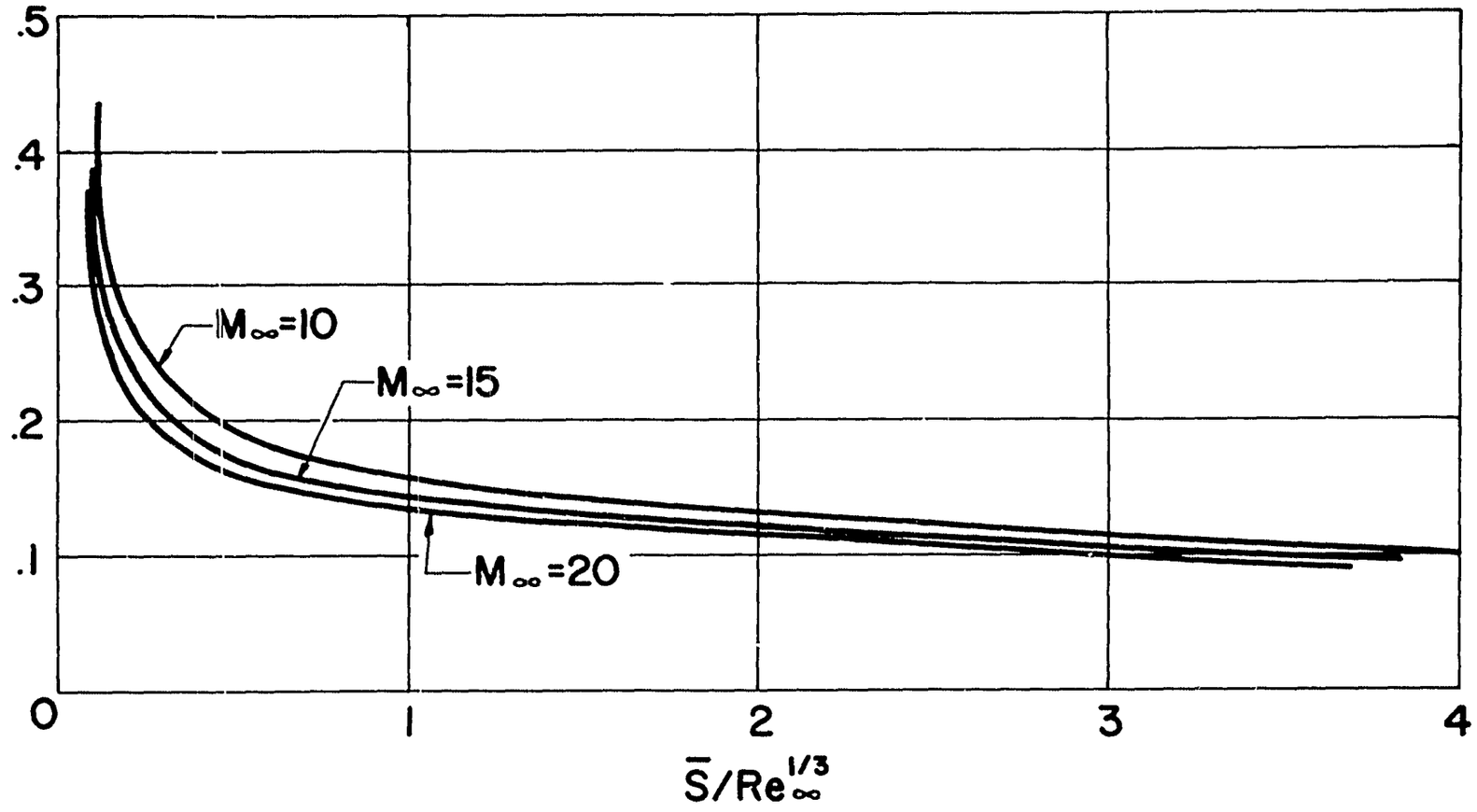

FIG. 12b HEAT TRANSFER PARAMETER $Nu/(R_{eol})^{1/3}$ AS A FUNCTION OF THE SIMILARITY PARAMETER $\bar{S}/R_{e\infty}^{1/3}$, $\theta_B = 10°$

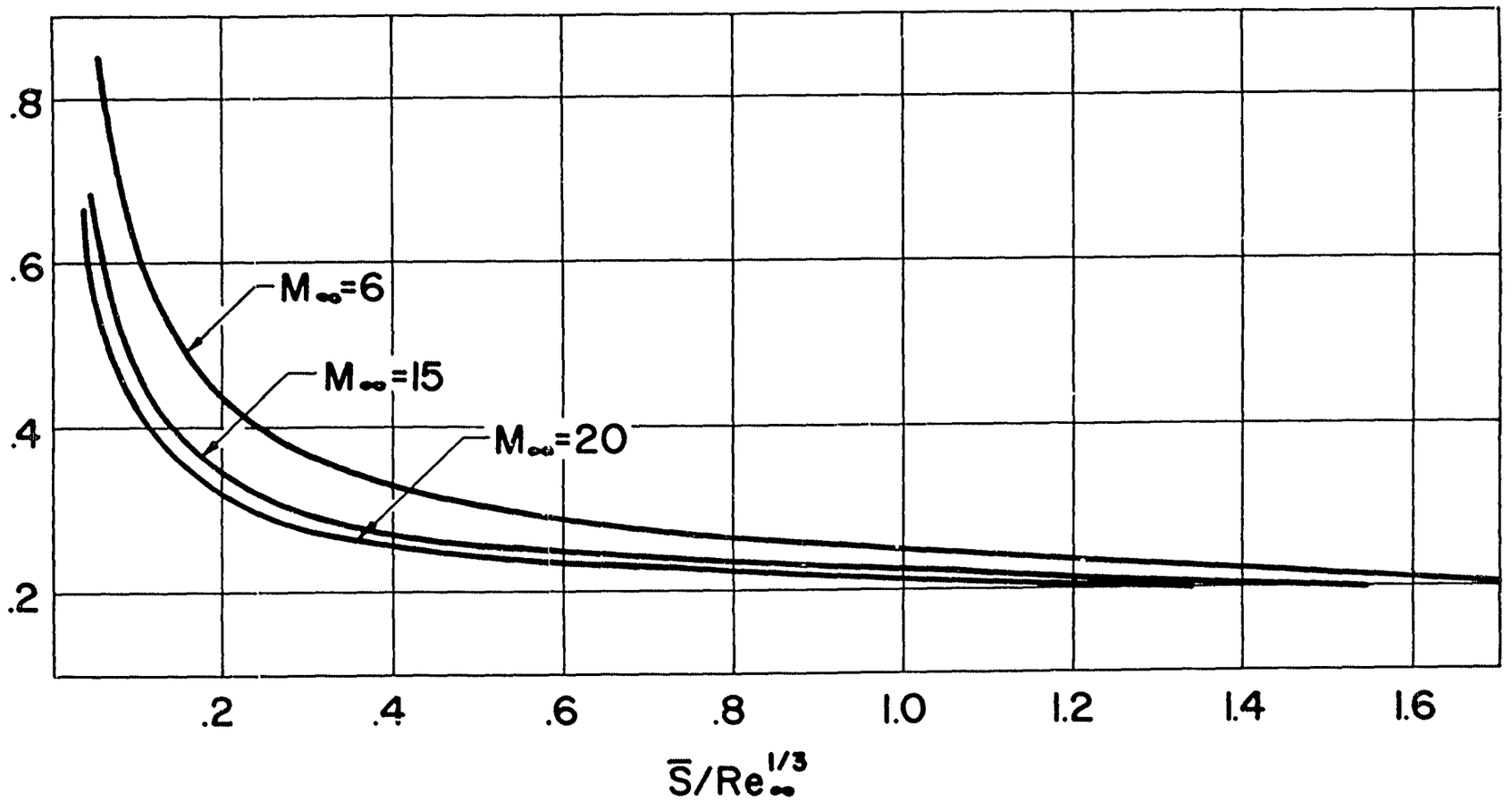

FIG. 12c HEAT TRANSFER PARAMETER $Nu/(R_{eol})^{1/3}$ AS A FUNCTION OF THE SIMILARITY PARAMETER $\bar{S}/R_{e\infty}^{1/3}$, $\theta_B = 15°$

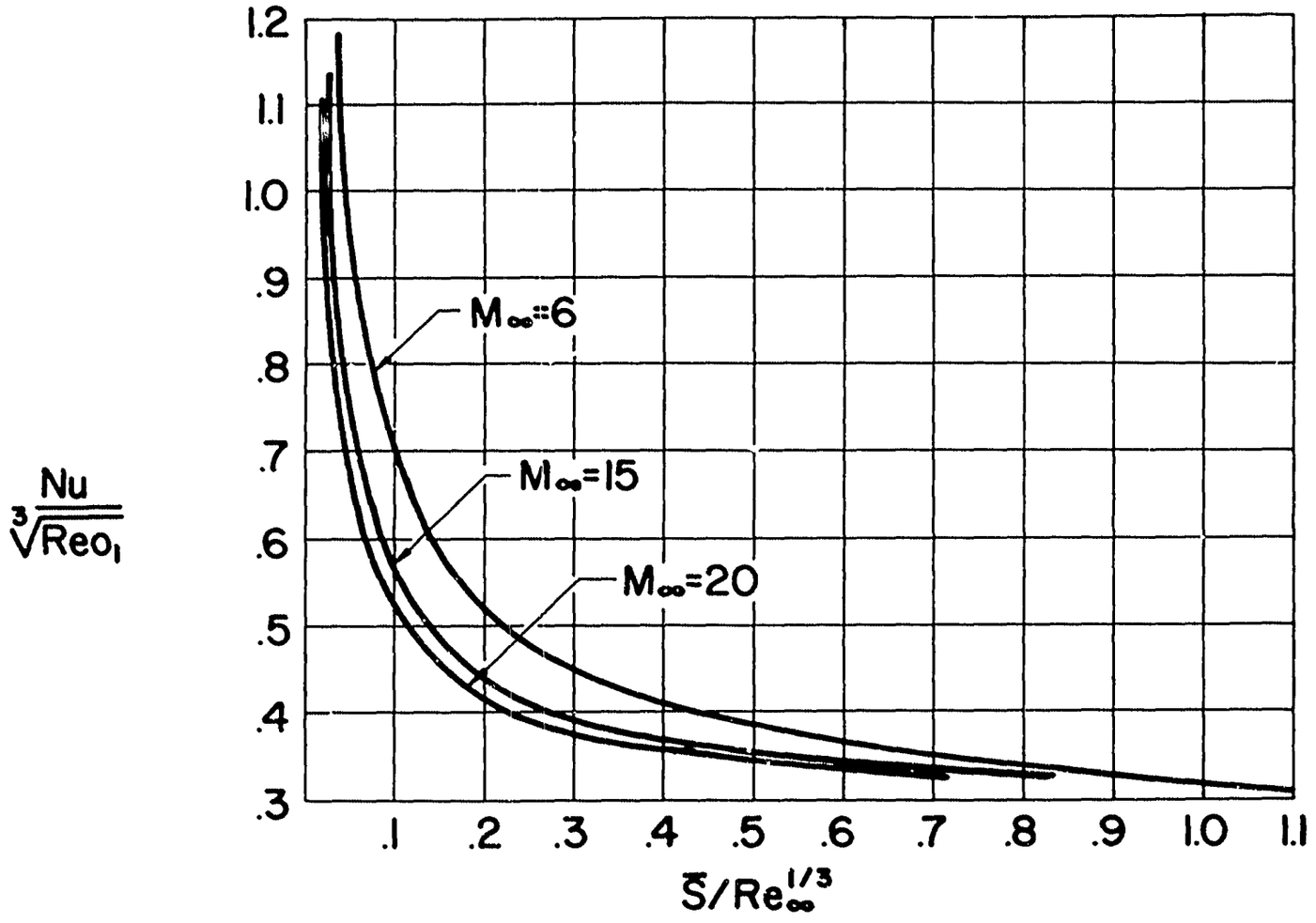

FIG. 12d HEAT TRANSFER PARAMETER $Nu/(R_{eol})^{1/3}$ AS A FUNCTION OF THE SIMILARITY PARAMETER $\bar{S}/R_{e\infty}^{1/3}$, $\theta_B = 20°$

Unclassified

Security Classification

DOCUMENT CONTROL DATA - R&D

(Security classification of title, body of abstract and indexing annotation must be entered when the overall report is classified)

1. ORIGINATING ACTIVITY (Corporate author)	2a. REPORT SECURITY CLASSIFICATION
New York University Bronx, New York 10453	Unclassified
	2b GROUP

3. REPORT TITLE

EFFECTS OF NOSE BLUNTNESS ON THE BOUNDARY LAYER CHARACTERISTICS OF CONICAL BODIES AT HYPERSONIC SPEEDS

4. DESCRIPTIVE NOTES (Type of report and inclusive dates)

Interim Report - November 1966

5. AUTHOR(S) (Last name, first name, initial)

Rotta, Nicholas, R.

6. REPORT DATE	7a. TOTAL NO. OF PAGES	7b. NO. OF REFS
November 1966	41	15

8a. CONTRACT OR GRANT NO.	9a. ORIGINATOR'S REPORT NUMBER(S)
NONR285(63)	NYU-AA-66-66
b. PROJECT NO. RR 009-02-01	
c.	9b. OTHER REPORT NO(S) (Any other numbers that may be assigned this report)
d.	none

10. AVAILABILITY/LIMITATION NOTICES

Distribution of this document is unlimited

11. SUPPLEMENTARY NOTES	12. SPONSORING MILITARY ACTIVITY
none	Department of the Navy Office of Naval Research Washington, D. C.

13. ABSTRACT

The effect of nose blunting on the boundary layer characteristics over the conical part of a body is investigated. The boundary layer parameters $\bar{\delta}^*$, $\bar{\theta}$, $R_{e\theta}$, $N_u/(R_{eol})^{\frac{1}{2}}$ are found as functions of the similarity parameter $\bar{s}/R_{e\infty}^{1/3}$, and the boundarylayer equations are integrated numerically. The resulting profiles are general, being independent of unit freestream Reynolds number and nose radius. The effect of bluntness on transition is investigated. Using the variation of Reynolds number based on the momentum thickness in the swallowing region as an indicator, the type of transition likely to occur, i.e., blunt body $R_{e\theta T} \approx 340$ or conical transition $R_{e\theta T} \approx 700$, is examined. The range of unit freestream Reynolds number for which conical transition will occur is identified specifically for the family of blunted conical bodies of 8° half angle at Mach 10. Based on the transition data, the heat transfer is calculated for regions of the swallowing process for which the boundary layer is laminar.

The results indicate a reduction of heat transfer is associated with nose bluntness and can be significant downstream of the nose region if the body nose radius is chosen to make the swallowing distance approximately twice that of the body surface length.

DD FORM 1 JAN 64 1473

Unclassified

Security Classification

14. KEY WORDS	LINK A		LINK B		LINK C	
	ROLE	WT	ROLE	WT	ROLE	WT
bluntness effects						
laminar boundary layer						
conical bodies						
hypersonic						
vorticity interaction						
heat transfer						

INSTRUCTIONS

1. ORIGINATING ACTIVITY: Enter the name and address of the contractor, subcontractor, grantee, Department of Defense activity or other organization *(corporate author)* issuing the report.

2a. REPORT SECURITY CLASSIFICATION: Enter the overall security classification of the report. Indicate whether "Restricted Data" is included. Marking is to be in accordance with appropriate security regulations.

2b. GROUP: Automatic downgrading is specified in DoD Directive 5200.10 and Armed Forces Industrial Manual. Enter the group number. Also, when applicable, show that optional markings have been used for Group 3 and Group 4 as authorized

3. REPORT TITLE: Enter the complete report title in all capital letters. Titles in all cases should be unclassified. If a meaningful title cannot be selected without classification, show title classification in all capitals in parenthesis immediately following the title.

4. DESCRIPTIVE NOTES: If appropriate, enter the type of report, e.g., interim, progress, summary, annual, or final. Give the inclusive dates when a specific reporting period is covered.

5. AUTHOR(S): Enter the name(s) of author(s) as shown on or in the report. Enter last name, first name, middle initial. If military, show rank and branch of service. The name of the principal author is an absolute minimum requirement.

6. REPORT DATE: Enter the date of the report as day, month, year, or month, year. If more than one date appears on the report, use date of publication.

7a. TOTAL NUMBER OF PAGES: The total page count should follow normal pagination procedures, i.e., enter the number of pages containing information.

7b. NUMBER OF REFERENCES: Enter the total number of references cited in the report.

8a. CONTRACT OR GRANT NUMBER: If appropriate, enter the applicable number of the contract or grant under which the report was written.

8b, 8c, & 8d. PROJECT NUMBER: Enter the appropriate military department identification, such as project number, subproject number, system numbers, task number, etc.

9a. ORIGINATOR'S REPORT NUMBER(S). Enter the official report number by which the document will be identified and controlled by the originating activity. This number must be unique to this report.

9b. OTHER REPORT NUMBER(S): If the report has been assigned any other report numbers *(either by the originator or by the sponsor)*, also enter this number(s).

10. AVAILABILITY/LIMITATION NOTICES: Enter any limitations on further dissemination of the report, other than those imposed by security classification, using standard statements such as:

(1) "Qualified requesters may obtain copies of this report from DDC."

(2) "Foreign announcement and dissemination of this report by DDC is not authorized."

(3) "U. S. Government agencies may obtain copies of this report directly from DDC. Other qualified DDC users shall request through _____."

(4) "U. S. military agencies may obtain copies of this report directly from DDC. Other qualified users shall request through _____."

(5) "All distribution of this report is controlled. Qualified DDC users shall request through _____."

If the report has been furnished to the Office of Technical Services, Department of Commerce, for sale to the public, indicate this fact and enter the price, if known.

11. SUPPLEMENTARY NOTES: Use for additional explanatory notes.

12. SPONSORING MILITARY ACTIVITY: Enter the name of the departmental project office or laboratory sponsoring *(paying for)* the research and development. Include address.

13 ABSTRACT: Enter an abstract giving a brief and factual summary of the document indicative of the report, even though it may also appear elsewhere in the body of the technical report. If additional space is required, a continuation sheet shall be attached.

It is highly desirable that the abstract of classified reports be unclassified. Each paragraph of the abstract shall end with an indication of the military security classification of the information in the paragraph, represented as *(TS)*, *(S)*, *(C)*, or *(U)*.

There is no limitation on the length of the abstract. However, the suggested length is from 150 to 225 words.

14. KEY WORDS: Key words are technically meaningful terms or short phrases that characterize a report and may be used as index entries for cataloging the report. Key words must be selected so that no security classification is required. Identifiers, such as equipment model designation, trade name, military project code name, geographic location, may be used as key words but will be followed by an indication of technical context. The assignment of links, roles, and weights is optional.